

# Ferromagnetism and giant magnetoresistance in the rare earth fullerides $\text{Eu}_{6-x}\text{Sr}_x\text{C}_{60}$

Kenji Ishii\*

*Department of Physics, School of Science, The University of Tokyo,  
7-3-1 Hongo, Bunkyo-ku, Tokyo 113-0033, Japan and  
Synchrotron Radiation Research Center, Kansai Research Establishment,  
Japan Atomic Energy Research Institute, 1-1-1 Kouto Mikazuki-cho Sayo-gun, Hyogo 679-5148, Japan*

Akihiko Fujiwara<sup>†</sup> and Hiroyoshi Suematsu<sup>‡</sup>

*Department of Physics, School of Science, The University of Tokyo,  
7-3-1 Hongo, Bunkyo-ku, Tokyo 113-0033, Japan*

Yoshihiro Kubozono

*Department of Chemistry, Faculty of Science, Okayama University,  
3-1-1 Tsushima-naka, Okayama 700-8530, Japan*

(Dated: October 25, 2018)

We have studied crystal structure, magnetism and electric transport properties of a europium fulleride  $\text{Eu}_6\text{C}_{60}$  and its Sr-substituted compounds,  $\text{Eu}_{6-x}\text{Sr}_x\text{C}_{60}$ . They have a *bcc* structure, which is an isostructure of other  $M_6\text{C}_{60}$  ( $M$  represents an alkali atom or an alkaline earth atom). Magnetic measurements revealed that magnetic moment is ascribed to the divalent europium atom with  $S = 7/2$  spin, and a ferromagnetic transition was observed at  $T_C = 10 - 14$  K. In  $\text{Eu}_6\text{C}_{60}$ , we also confirm the ferromagnetic transition by heat capacity measurement. The striking feature in  $\text{Eu}_{6-x}\text{Sr}_x\text{C}_{60}$  is very large negative magnetoresistance at low temperature; the resistivity ratio  $\rho(H = 9 \text{ T})/\rho(H = 0 \text{ T})$  reaches almost  $10^{-3}$  at 1 K in  $\text{Eu}_6\text{C}_{60}$ . Such large magnetoresistance is the manifestation of a strong  $\pi$ - $f$  interaction between conduction carriers on  $\text{C}_{60}$  and  $4f$  electrons of Eu.

PACS numbers: 61.48.+c, 75.50.-y, 72.80.Rj, 61.10.-i

## I. INTRODUCTION

Since the discovery of fullerenes,  $\text{C}_{60}$  compounds have given us various opportunities for the research in condensed matter physics and materials science. Much attention was attracted to the superconductivity in  $A_3\text{C}_{60}$  ( $A$  is an alkali atom)<sup>1</sup>. As for the magnetism, TDAE- $\text{C}_{60}$  (TDAE is tetrakisdimethylaminoethylene) shows a ferromagnetic transition<sup>2</sup>, while antiferromagnetic (or spin density wave) ground state was observed in polymeric  $A_1\text{C}_{60}$ <sup>3</sup>,  $\text{Na}_2\text{Rb}_{0.3}\text{Cs}_{0.7}\text{C}_{60}$ <sup>4</sup>, and three-dimensional  $(\text{NH}_3)_A_3\text{C}_{60}$ <sup>5</sup>. In these compounds a magnetic moment is considered to be carried by an electron on  $\text{C}_{60}$  molecule. Because various atoms and molecules can be intercalated into  $\text{C}_{60}$  crystal, we also expect the magnetic  $\text{C}_{60}$  compounds in which magnetic moment is carried by intercalants. In this viewpoint, rare earth metal is a good candidate. The research of rare earth fullerides was reported for Yb<sup>6</sup> and Sm<sup>7</sup> in relation to the superconductivity, but little effort has been made to study the magnetic properties. The only case of magnetic study in rare earth fullerides is for europium. Europium has a magnetic moment of  $7\mu_B$  ( $S = 7/2$ ,  $L = 0$ , and  $J = 7/2$ ) in the divalent state, while it is non-magnetic ( $S = 3$ ,  $L = 3$ , and  $J = 0$ ) in the trivalent state. A photoemission study of  $\text{C}_{60}$  overlaid on Eu metal revealed the charge transfer from Eu to  $\text{C}_{60}$  and the formation of fulleride<sup>8</sup>. Ksari-Habiles *et al.*<sup>9,10</sup> investigated the crystal structure and magnetic properties of  $\text{Eu}_{\sim 3}\text{C}_{60}$  and  $\text{Eu}_6\text{C}_{60}$ ; they observed some magnetic anomalies in  $\text{Eu}_6\text{C}_{60}$ .

In this paper, we report the ferromagnetic transition of  $\text{Eu}_6\text{C}_{60}$ , which was observed at  $T_C \sim 12$  K in magnetic and heat capacity measurements. We also investigated the substitution effect from Eu to non-magnetic Sr, and the ferromagnetic transition temperature was found to change little with the Sr concentration. In the resistivity measurement we found a huge negative magnetoresistance below around  $T_C$ ; the reduction ratio of resistivity  $\rho(H)/\rho(0)$  is almost  $10^{-3}$  at 1 K in  $\text{Eu}_6\text{C}_{60}$ . This ratio is comparable to those in perovskite manganese oxides, which is known as colossal magnetoresistance (CMR). However  $\text{Eu}_6\text{C}_{60}$  should be categorized as a new class of giant magnetoresistive compounds in the sense that (1) the magnitude of magnetoresistance increases very steeply with decreasing temperature rather than the vicinity of  $T_C$ , (2) the compound consists of a molecule with novel structure. These features can open the further possibility to find a new magnetic and magnetoresistive material.

## II. EXPERIMENTAL PROCEDURES

Polycrystalline samples of  $\text{Eu}_{6-x}\text{Sr}_x\text{C}_{60}$  were synthesized by solid-state reaction. A stoichiometric amount of mixture of Eu, Sr and  $\text{C}_{60}$  powders, which was pressed into a pellet and sealed in a quartz tube in vacuum, was heat-treated at 600 °C for about 10 days. In the course of the heat treatment the sample was ground for ensuring the complete reaction. Because the sample is very

unstable in air, we treated it in a glove box with inert atmosphere.

Powder x-ray diffraction experiments were carried out by using synchrotron radiation x-rays at BL-1B in Photon Factory, KEK, Tsukuba. The samples was put into a glass capillary in 0.3 mm diameter and an imaging plate was used for the detection<sup>11</sup>. Magnetic measurements were performed using a SQUID magnetometer. In the heat capacity measurement by relaxation method, the sample was pressed into a pellet and sealed by grease to keep from exposure to air. Eu  $L_{III}$ -edge XANES (x-ray absorption near edge structure) was measured in the fluorescence method at BL01B1 of SPring-8, Harima. The resistivity measurements were carried out by the 4-probe method. Four gold wires were attached to a pressed pellet of polycrystalline sample with sliver paste. The sample was put into a capsule and sealed in He atmosphere.

### III. RESULTS

X-ray diffraction spectra of  $\text{Eu}_{6-x}\text{Sr}_x\text{C}_{60}$  are shown in Fig. 1(a). The spectrum of  $\text{Sr}_6\text{C}_{60}$  is also presented as a reference. The wavelength of x-ray is 0.8057 Å for  $x = 0, 3, 5$ , and 0.8011 Å for  $x = 6$ . They all can be understood by a  $bcc$  structure which is an isostructure of other  $M_6\text{C}_{60}$  in alkali<sup>12</sup>, alkaline earth<sup>13</sup> and rare earth (Sm)<sup>14</sup> fullerenes. The Rietveld refinements based on the space group  $Im\bar{3}$  were performed with use of the RIETAN program<sup>15,16</sup>. In the refinements, only two atomic coordinates ( $x$  for C1 and C3) are refined in  $\text{C}_{60}$  molecule, which corresponds to the refinement of the length of 6:6 bond (the bond between two hexagons) and 5:6 bond (the bond between hexagon and pentagon). In the compounds of  $x = 3$  and 5, the sum of the metal concentration is fixed to unity. The results of refinement are presented in Table I and obtained structure is shown in Fig. 1(b). This crystal structure of  $\text{Eu}_6\text{C}_{60}$  is consistent with the previous works<sup>10,17</sup>, but we observed little trace of the secondary phase in the present sample. In the Sr-substituted compounds, the values of Eu concentration are in good agreement with the nominal ones.

As seen in Fig. 1(c), the obtained lattice constants change linearly with the nominal Eu concentration, which means they follow the Vegard's law, and confirms the formation of solid solution at  $x = 3$  and 5. This result is attributed to the fact that ionic radius of  $\text{Eu}^{2+}$  and  $\text{Sr}^{2+}$  is quite similar, while the substitution of Ba for Eu results in the phase separation.

Figures 2 show the result of magnetic measurements of  $\text{Eu}_{6-x}\text{Sr}_x\text{C}_{60}$ . Above 30 K, magnetic susceptibility ( $\chi$ ) follows the Curie-Weiss law, as shown in Figs. 2(a)-(c). The effective Bohr magneton estimated from Curie constant and the Weiss temperature are summarized in Table II<sup>18</sup>. The former agrees with the  $\text{Eu}^{2+}$  state ( $S = 7/2$ ,  $L = 0$ , and  $J = 0$ ). The field dependence of magnetization at 2 K gives the saturation moment close to  $7\mu_B$ , which is consistent with the magnetic moment of

$\text{Eu}^{2+}$ . Moreover the  $\text{Eu}^{2+}$  state has been also confirmed by Eu  $L_{III}$ -edge XANES experiments, as seen in Fig. 3. The spectra of  $\text{EuS}$  and  $\text{Eu}_2\text{O}_3$  was also presented as a reference of divalent and trivalent of Eu, and absorption edges of  $\text{Eu}_{6-x}\text{Sr}_x\text{C}_{60}$  are very close to that of  $\text{EuS}$ . The divalent state of Eu also observed in the case that Eu atom exists inside the  $\text{C}_{60}$  cage, namely, metallofullerene  $\text{Eu}@\text{C}_{60}$ <sup>19</sup>.

Temperature dependence of magnetization at a weak field of 3 mT (Figs. 2(g)-(i)) shows a steep increase of magnetization below 10-14 K, indicating a ferromagnetic transition. To confirm the presence of the ferromagnetic phase transition, we measured heat capacity for  $\text{Eu}_6\text{C}_{60}$ . In Fig. 2(g) we show the temperature dependence of heat capacity including that of grease. An obvious peak can be seen near the transition temperature, which is an evidence of the ferromagnetic phase transition. The  $T_C$  is determined to be 11.6 K from the peak position. We ascertained that there was no anomaly in specific heat in this temperature region for grease, which was used to keep the sample from exposure to air. We can also see a smaller peak near 16 K, whose origin has not been clarified yet, but we consider that it does not come from a magnetic origin because of no anomaly in the temperature dependence of magnetization. The transition temperatures for  $\text{Eu}_3\text{Sr}_3\text{C}_{60}$  and  $\text{Eu}_1\text{Sr}_5\text{C}_{60}$  are estimated from the Arrott plot<sup>20</sup> at 12.8 K and 10.4 K, respectively. These values are very close to the Weiss temperature mentioned above. In  $\text{Eu}_6\text{C}_{60}$ , the transition temperature estimated from the Arrott plot is a little larger value (13.7 K) than that from the heat capacity measurement, but it is not so important in the following discussion.

From these evidences we conclude that  $\text{Eu}_{6-x}\text{Sr}_x\text{C}_{60}$  shows a ferromagnetic transition at  $T_C = 10-14$  K, and the magnetic moment is ascribed to  $\text{Eu}^{2+}$ . In the previous work of  $\text{Eu}_6\text{C}_{60}$ , Ksari-Habiles *et al.*<sup>9</sup> observed a mixed valence state of Eu ( $\text{Eu}^{2+}$  and  $\text{Eu}^{3+}$ ) and three successive magnetic anomalies, which is different from the present work; a possible reason is that their sample might contain a secondary phase other than  $\text{Eu}_6\text{C}_{60}$ .

Figure 4 (a) show the temperature dependence of electric resistivity of  $\text{Eu}_6\text{C}_{60}$  measured at some magnetic fields. A most striking feature in resistivity is the huge negative magnetoresistance below around  $T_C$ . The negative magnetoresistance becomes much more significant at lower temperature. In the case of  $\text{Eu}_6\text{C}_{60}$ , magnetoresistivity  $\rho(H = 9 \text{ T})$  is three orders magnitude smaller than  $\rho(H = 0 \text{ T})$  at 1 K, as seen in Fig. 4 (b). This large negative magnetoresistance is comparable to those of the colossal magnetoresistance (CMR) materials such as perovskite manganese oxides, where CMR effect is seen only near the ferromagnetic transition temperature. We also observed a relatively large magnetoresistance in the Sr-substituted compounds, as shown in 4 (c). There is no difference between magnetoresistances in the transverse ( $H \perp I$ ) and longitudinal ( $H \parallel I$ ) configurations ( $I$  represents electric current), suggesting the magnetoresistance

in  $\text{Eu}_6\text{C}_{60}$  is not ascribed to the orbital motion of free carriers.

#### IV. DISCUSSION

Such giant magnetoresistance is a manifestation of the strong interaction between conduction carriers and localized magnetic moments; namely, the strong  $\pi$ - $f$  interaction exists in  $\text{Eu}_6\text{C}_{60}$ . When we consider formal valence state of  $(\text{Eu}^{2+})_6\text{C}_{60}^{12-}$ ,  $t_{1g}$  band of  $\text{C}_{60}$  is completely filled and the compound should become an insulator. In this case, the interaction between conduction carrier and localized moment is considered to be weak, assuming that the conduction carrier mainly passes on  $\text{C}_{60}$  molecules. If Eu orbitals hybridize with  $\text{C}_{60}$  orbitals and form a part of conduction band, much enhancement of the interaction must occur. In the band calculation for  $\text{Sr}_6\text{C}_{60}$  and  $\text{Ba}_6\text{C}_{60}$ <sup>21</sup> which have the same *bcc* crystal structure and the same valence state as  $\text{Eu}_6\text{C}_{60}$ , the hybridization of the  $d$  orbital of metal atom and the  $t_{1g}$  orbital of  $\text{C}_{60}$  exists and make the compounds metallic. This fact is confirmed experimentally<sup>22</sup>. The hybridization is more significant in  $\text{Sr}_6\text{C}_{60}$  than  $\text{Ba}_6\text{C}_{60}$  due to the smaller lattice constant of  $\text{Sr}_6\text{C}_{60}$ . The band structure of  $\text{Eu}_6\text{C}_{60}$  has not been studied yet, but such hybridization of the  $5d$  and/or  $6s$  orbitals of Eu and the  $t_{1g}$  orbital of  $\text{C}_{60}$  is plausible in  $\text{Eu}_6\text{C}_{60}$  because  $\text{Eu}_6\text{C}_{60}$  has a further smaller lattice constant than  $\text{Sr}_6\text{C}_{60}$ .

The  $\pi$ - $f$  interaction is likely to affect to magnetic interaction of  $4f$  electrons and the origin of ferromagnetism in  $\text{Eu}_6\text{C}_{60}$  may be ascribed to the indirect exchange interaction. In the *bcc* structure, an Eu atom has 4 nearest neighbor Eu atoms (the distance between two Eu atoms is 3.89 Å). Therefore, in the case of  $\text{Eu}_1\text{Sr}_5\text{C}_{60}$ , 5 of 6 Eu atoms are replaced by non-magnetic Sr atoms, Eu atoms can no longer have the three-dimensional Eu network, so that the direct interaction fails completely. Nevertheless  $T_C$  does not show a drastic change. This is a quite contrast with the case of magnetic semiconductor EuO, where the direct exchange interaction between Eu atoms is important<sup>23</sup> and the substitution of Ca for Eu significantly reduces the ferromagnetic transition temperature<sup>24</sup>. This fact indicates that the ferromagnetism in  $\text{Eu}_6\text{C}_{60}$  comes from the indirect exchange interaction via  $\text{C}_{60}$  molecules, and the  $\pi$ - $f$  interaction has an important role in the present system.

Now we discuss the origin of the giant magnetoresistance. The features of magnetoresistance in  $\text{Eu}_6\text{C}_{60}$  are (1) negative magnetoresistance occurs below around  $T_C$ , (2) saturation field of magnetization is close to that of magnetoresistance ratio ( $\rho(H)/\rho(0)$ ), as seen in the top curve of Fig. 2(d) and the bottom curve of Fig. 4(c), (3) magnetoresistance is much enhanced at lower temperatures; The magnetoresistance ratio ( $\rho(H)/\rho(0)$ ) does not seem to saturate with decreasing temperature, while the magnetization almost saturates at 2 K and 5.5 T. The feature (1) indicates that the present MR is closely

related to the ferromagnetic transition. In usual ferromagnetic metal, spin fluctuation scatters conduction electrons and causes negative magnetoresistance<sup>25,26</sup>. This effect may be an origin of the magnetoresistance near  $T_C$ , but this is not the case for the giant magnetoresistance in  $\text{Eu}_6\text{C}_{60}$  at lower temperature, because such effect is remarkable in the vicinity of  $T_C$  inconsistent with the feature (3). The feature (2) suggests that magnetoresistance is related to the magnetization. Furthermore, when we see  $\rho(H)/\rho(0)$  in log scale, the difference of  $\rho(H)/\rho(0)$  between 2 K and 1 K is almost one order (Fig. 4(b)), while that of magnetization must be small. This means there is another factor, in addition to the magnetization, to determine the magnetoresistance. It is probably temperature, that is, an activation process needs to be considered in the origin of the magnetoresistance.

One possible interpretation of magnetoresistance in  $\text{Eu}_6\text{C}_{60}$  is the spin-dependent tunneling at the grain boundary<sup>27</sup>. In the case of ferromagnetic granular metal, the conductivity is dependent on the tunneling probability of carriers through insulating barrier between grains, and the probability crucially depends on the spin polarization of carriers. In this case, each grain is assumed to be conductive and surrounded by less conductive surface. Because we measured the resistivity in a pellet of polycrystalline sample and  $\text{Eu}_6\text{C}_{60}$  is very unstable in air, the surface may react to be insulative barrier, even if the sample is treated in high purity inert atmosphere. However we should note that the insulating region is considered to be limited only on the thin surface because unidentified peaks in XRD spectrum are very weak and they are considered not to affect to the magnetic and heat capacity measurements. As shown in the inset of Fig. 4(a), the temperature dependence of resistivity is represented as  $\rho(T) \propto \exp(T_0/T)^{1/\alpha}$  ( $\alpha \sim 2$ ), rather than the activation type which is expected in a usual semiconductor. The value of  $T_0$  is about 180 K at 0T. This fact suggests that the resistivity in our sample might be governed by the tunneling at the boundaries<sup>28</sup>. Our preliminary Hall effect measurement gives  $R_H = +5 \times 10^{-2} \text{ cm}^3/\text{C}$  at 250 K, corresponding to the hole density of  $1 \times 10^{20} \text{ cm}^{-3}$  (0.1 hole per  $\text{C}_{60}$ ); this means that intrinsic  $\text{Eu}_6\text{C}_{60}$  can have relatively high conductivity and is possibly metallic by hybridization of the  $\text{C}_{60}$  and metal orbitals mentioned above. Note that Hall voltage is less sensitive to the grain boundary effect. Helman and Abeles<sup>27</sup> considered the magnetic exchange energy  $E_M$  and gave the magnetoresistance of orders of magnitude only when  $P$  is very

$$\sigma(H, T) = \sigma_0 [\cosh(E_M/2k_B T) - P \sinh(E_M/2k_B T)], \quad (1)$$

where  $P$  is the spin polarization of carrier and  $E_M = (1/2)J[1 - m^2]$ .  $J$  is the exchange coupling constant between a conduction carrier and a ferromagnetic metal grain and  $m$  is the magnetization normalized by the saturation value. The equation (1) gives a negative magnetoresistance of orders of magnitude only when  $P$  is very

close to unity. If  $P = 1$ , we obtain

$$\rho(H)/\rho(0) = \exp(-Jm^2/4k_B T). \quad (2)$$

Magnetoresistance in equation (2) becomes large with decreasing temperature, which agree qualitatively with the feature (2) mentioned above. The assumption of  $P = 1$  might be unrealistic in usual ferromagnetic metals. However, if the exchange interaction between Eu atoms is accomplished via  $\pi$ -bands of  $C_{60}$  as discussed earlier, we can expect a large spin polarization of  $\pi$ -electrons.

We can also consider the effect of magnetic polaron. In magnetic semiconductors such as Eu chalcogenides, a carrier makes surrounding magnetic moments be polarized via exchange interaction and forms a magnetic polaron<sup>29</sup>. At zero field, magnetic polarons have to move with flipping some magnetic moments which are more or less randomly oriented, and their conduction is suppressed. Application of magnetic field aligns spin directions and carriers become mobile. As a result, negative magnetoresistance occurs. The negative magnetoresistance above  $T_C$  can be attributed to this picture. Even in the ferromagnetic phase, magnetic moments have to be flipped at a magnetic domain boundary for the motion of carrier. Because remnant magnetic moment is little, as seen in Figs. 2 (d), many magnetic domains exist in our sample of  $Eu_6C_{60}$ . The crucial point of above two interpretations (spin dependent tunneling and magnetic polaron) are that carriers must overcome large exchange interaction with localized spins when they go into the region of different orientation of magnetic moments.

## V. SUMMARY

We have measured crystal structure, magnetic properties and magnetoresistance in polycrystalline  $Eu_6C_{60}$  and its Sr-substituted compounds,  $Eu_{6-x}Sr_xC_{60}$ . They all have a *bcc* structure and the compounds of  $x = 3$  and 5 form a solid solution concerning the occupation of metal atom. A ferromagnetic transition is observed at  $T_C \sim 12$  K in  $Eu_6C_{60}$  and all Eu atoms are in divalent state with a magnetic moment of  $7\mu_B$  ( $S = 7/2$ ). The fact that the substitution of non-magnetic Sr for Eu affects little to  $T_C$  indicates the ferromagnetic interaction is caused through the conduction carriers. In the resistivity measurement, we have found that  $Eu_6C_{60}$  showed a huge negative magnetoresistance and  $\rho(H)/\rho(0)$  reduced almost  $10^{-3}$  at  $H = 9$  T and  $T = 1$  K. The precise mechanism of magnetoresistance has not clarified yet, but it manifests a strong interaction between  $\pi$ -conduction electrons of  $C_{60}$  and  $4f$  electrons on Eu.

## Acknowledgments

We acknowledge to Prof. Y. Iwasa, Dr. T. Takenobu and S. Moriyama for the suggestions for synthesis and heat capacity measurements. We also thank to Prof. A. Asamitsu for the advice of the resistivity measurements at low temperature. This work was supported by ‘‘Research for the Future’’ of Japan Society for the Promotion of Science (JSPS), Japan.

\* Electronic address: kenji@spring8.or.jp

† Present address: School of Materials Science, Japan Advanced Institute of Science and Technology, 1-1 Asahidai, Tatsunokuchi, Ishikawa 923-1292, Japan

‡ Present address: Material Science Division, SR Research Laboratory, Japan Synchrotron Radiation Research Institute, 1-1-1 Kouto Mikazuki-cho, Sayo-gun, Hyogo 679-5198, Japan

<sup>1</sup> A. F. Hebard, M. J. Rosseinsky, R. C. Haddon, D. W. Murphy, S. H. Glarum, T. T. M. Palstra, A. P. Ramirez, and A. R. Kortan, *Nature (London)* **350**, 600 (1991).

<sup>2</sup> P. M. Allemand, K. C. Khemani, A. Koch, F. Wudl, K. Holczer, S. Donovan, G. Grüner, and J. D. Thompson, *Science* **253**, 301 (1991).

<sup>3</sup> O. Chauvet, G. Oszlányi, L. Forro, P. W. Stephens, M. Tegze, G. Faigel, and A. Jánossy, *Phys. Rev. Lett.* **72**, 2721 (1994).

<sup>4</sup> D. Arçon, K. Prassides, A. L. Maniero, and L. C. Brunel, *Phys. Rev. Lett.* **84**, 562 (2000).

<sup>5</sup> T. Takenobu, T. Muro, Y. Iwasa, and T. Mitani, *Phys. Rev. Lett.* **85**, 381 (2000).

<sup>6</sup> E. Özdaş, A. R. Kortan, N. Kopylov, A. P. Ramirez, T. Siegrist, K. M. Rabe, H. E. Bair, S. Schuppler, and P. H. Citrin, *Nature (London)* **375**, 126 (1995).

<sup>7</sup> X. H. Chen and G. Roth, *Phys. Rev. B* **52**, 15534 (1995).

<sup>8</sup> H. Yoshikawa, S. Kuroshima, I. Hirosawa, K. Tanigaki, ,

and J. Mizuki, *Chem. Phys. Lett.* **239**, 103 (1995).

<sup>9</sup> Y. Ksari-Habiles, D. Claves, G. Chouteau, P. Touzain, C. Jeandey, J. L. Odoou, and A. Stepanov, *J. Phys. Chem. Solids* **58**, 1771 (1997).

<sup>10</sup> D. Claves, Y. Ksari-Habiles, G. Chouteau, and P. Touzain, *Solid State Commun.* **106**, 431 (1998).

<sup>11</sup> A. Fujiwara, K. Ishii, T. Watanuki, H. Suematsu, H. Nakao, K. Ohwada, Y. Fujii, Y. Murakami, T. Mori, H. Kawada, et al., *J. Appl. Cryst.* **33**, 1241 (2000).

<sup>12</sup> O. Zhou, J. E. Fisher, N. Coustel, S. Kycia, Q. Zhu, A. R. McGhie, W. J. Romanow, J. P. M. Jr., A. B. S. III, and D. E. Cox, *Nature (London)* **351**, 462 (1991).

<sup>13</sup> A. R. Kortan, N. Kopylov, S. Glarum, E. M. Gyorgy, A. P. Ramirez, R. M. Fleming, O. Zhou, F. A. Thiel, P. L. Trevor, and R. C. Haddon, *Nature (London)* **360**, 566 (1991).

<sup>14</sup> X. H. Chen, Z. S. Liu, S. Y. Li, D. H. Chi, and Y. Iwasa, *Phys. Rev. B* **60**, 6183 (1999).

<sup>15</sup> F. Izumi, in *The Rietveld Method*, edited by R. A. Young (Oxford University Press, Oxford, 1993), chap. 13.

<sup>16</sup> Y. I. Kim and F. Izumi, *J. Ceram. Soc. Jpn.* **102**, 401 (1994).

<sup>17</sup> H. Ootoshi, K. Ishii, A. Fujiwara, T. Watanuki, Y. Matsuoka, and H. Suematsu, *Mol Cryst. and Liq. Cryst.* **340**, 565 (2000).

<sup>18</sup> In  $Eu_3Sr_3C60$  and  $Eu_1Sr_5C60$ , the values of  $\mu_{eff}$  and  $M_S$

in Tabel II are a little larger than the theoretical values of  $\text{Eu}^{2+}$ . The most probable reason is the discrepancy of the stoichiometry, but the excess from the theoretical value is often observed in the samples of different batches, including  $\text{Eu}_6\text{C}_{60}$ .

- <sup>19</sup> T. Inoue, Y. Kubozono, S. Kashino, Y. Takabayashi, K. Fujitaka, M. Hida, M. Inoue, T. Kambara, S. Emura, and T. Uruga, Chem. Phys. Lett. **316**, 381 (2000).  
<sup>20</sup> A. Arrott, Phys. Rev. **108**, 1394 (1957).  
<sup>21</sup> S. Saito and A. Oshiyama, Phys. Rev. Lett. **71**, 121 (1993).  
<sup>22</sup> B. Gogia, K. Kordatos, H. Suematsu, K. Tanigaki, and K. Prassides, Phys. Rev. B **58**, 1077 (1998).  
<sup>23</sup> T. Kasuya, I.B.M. J. Res. Develop. **14**, 214 (1970).  
<sup>24</sup> A. A. Samokhvalov, N. N. Loshkareva, and V. G. Bamburov, Sov. Phys. Solid State **9**, 555 (1967).  
<sup>25</sup> P. G. E. de Gennes and J. Friedel, J. of Phys. Chem. Solids **4**, 71 (1958).  
<sup>26</sup> M. E. Fisher and J. S. Langer, Phys. Rev. Lett. **20**, 665 (1968).  
<sup>27</sup> J. S. Helman and B. Abeles, Phys. Rev. Lett. **37**, 1429 (1976).  
<sup>28</sup> P. Sheng, B. Abeles, and Y. Arie, Phys. Rev. Lett. **31**, 44 (1972).  
<sup>29</sup> T. Kasuya and A. Yanase, Rev. Mod. Phys. **40**, 684 (1968).

TABLE I: Structural parameter obtained from the Rietveld refinement of  $\text{Eu}_{6-x}\text{Sr}_x\text{C}_{60}$ .

Eu <sub>6</sub> C <sub>60</sub> $a_0 = 10.940 \pm 0.001 \text{ \AA}$ $R_{wp} = 3.81 \%$						
Site	Occupancy	$x$	$y$	$z$	$B(\text{\AA}^2)$	
C1	24g	1	0.0672(5)	0	0.3200	0.5(2)
C2	48h	1	0.1325	0.1056	0.2797	0.5
C3	48h	1	0.0653(3)	0.2144	0.2381	0.5
Eu <sup>2+</sup>	12e	1	0	0.5	0.2768(2)	2.29(4)
Eu <sub>3</sub> Sr <sub>3</sub> C <sub>60</sub> $a_0 = 10.958 \pm 0.002 \text{ \AA}$ $R_{wp} = 6.20 \%$						
Site	Occupancy	$x$	$y$	$z$	$B(\text{\AA}^2)$	
C1	24g	1	0.0686(6)	0	0.3186	1.1(3)
C2	48h	1	0.1328	0.1038	0.2790	1.1
C3	48h	1	0.0641(4)	0.2148	0.2366	1.1
Eu <sup>2+</sup>	12e	0.51(2)	0	0.5	0.2792(3)	2.99(7)
Sr <sup>2+</sup>	12e	0.49	0	0.5	0.2792	2.99
Eu <sub>1</sub> Sr <sub>5</sub> C <sub>60</sub> $a_0 = 10.971 \pm 0.002 \text{ \AA}$ $R_{wp} = 6.37 \%$						
Site	Occupancy	$x$	$y$	$z$	$B(\text{\AA}^2)$	
C1	24g	1	0.0660(5)	0	0.3207	2.1(3)
C2	48h	1	0.1321	0.1069	0.2798	2.1
C3	48h	1	0.0661(3)	0.2138	0.2390	2.1
Eu <sup>2+</sup>	12e	0.18(2)	0	0.5	0.2803(3)	2.73(6)
Sr <sup>2+</sup>	12e	0.82	0	0.5	0.2803(3)	2.73
Sr <sub>6</sub> C <sub>60</sub> $a_0 = 10.986 \pm 0.002 \text{ \AA}$						

TABLE II: Summary of the magnetic properties of  $\text{Eu}_{6-x}\text{Sr}_x\text{C}_{60}$ .  $\mu_{eff}$ ,  $\Theta$ ,  $M_S$ , and  $T_C$  denote effective Bohr magneton ( $gJ\sqrt{J(J+1)}\mu_B$ ), Weiss temperature, saturation moment, and ferromagnetic transition temperature, respectively.

	$\mu_{eff}/\text{Eu} (\mu_B)$	$\Theta$ (K)	$M_S/\text{Eu} (\mu_B)$	$T_C$ (K)
Eu <sup>2+</sup>	7.94		7	
Eu <sub>6</sub> C <sub>60</sub>	7.77	10.6	6.97	11.6 <sup>a</sup> (13.7 <sup>b</sup> )
Eu <sub>3</sub> Sr <sub>3</sub> C <sub>60</sub>	8.13	12.6	7.73	12.8 <sup>b</sup>
Eu <sub>1</sub> Sr <sub>5</sub> C <sub>60</sub>	8.26	8.0	7.68	10.4 <sup>b</sup>

<sup>a</sup>From the peak position of heat capacity measurement.

<sup>b</sup>From the Arrott plot.

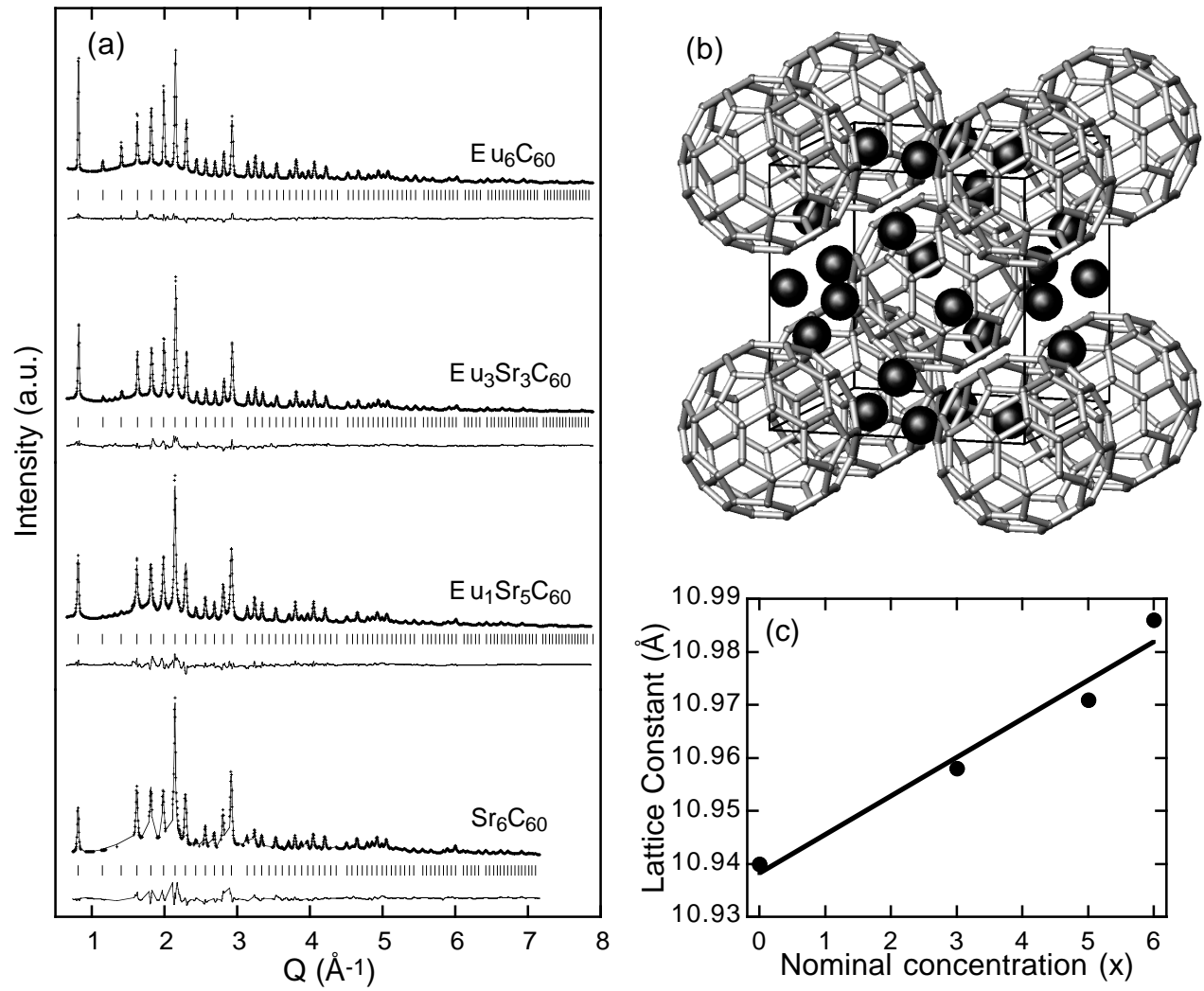


FIG. 1: (a) X-ray diffraction spectra of  $\text{Eu}_{6-x}\text{Sr}_x\text{C}_{60}$ . The wavelength of x-ray is  $0.8057 \text{ \AA}$  for  $x = 0, 3, 5$ , and  $0.8011 \text{ \AA}$  for  $x = 6$ . (b) Schematic view of the crystal structure of  $\text{Eu}_{6-x}\text{Sr}_x\text{C}_{60}$ . The black ball represents a metal atom. (c) Lattice constant vs. nominal concentration of Eu ( $x$ ). The lattice constant changes linearly with  $x$ , following the Vegard's law.

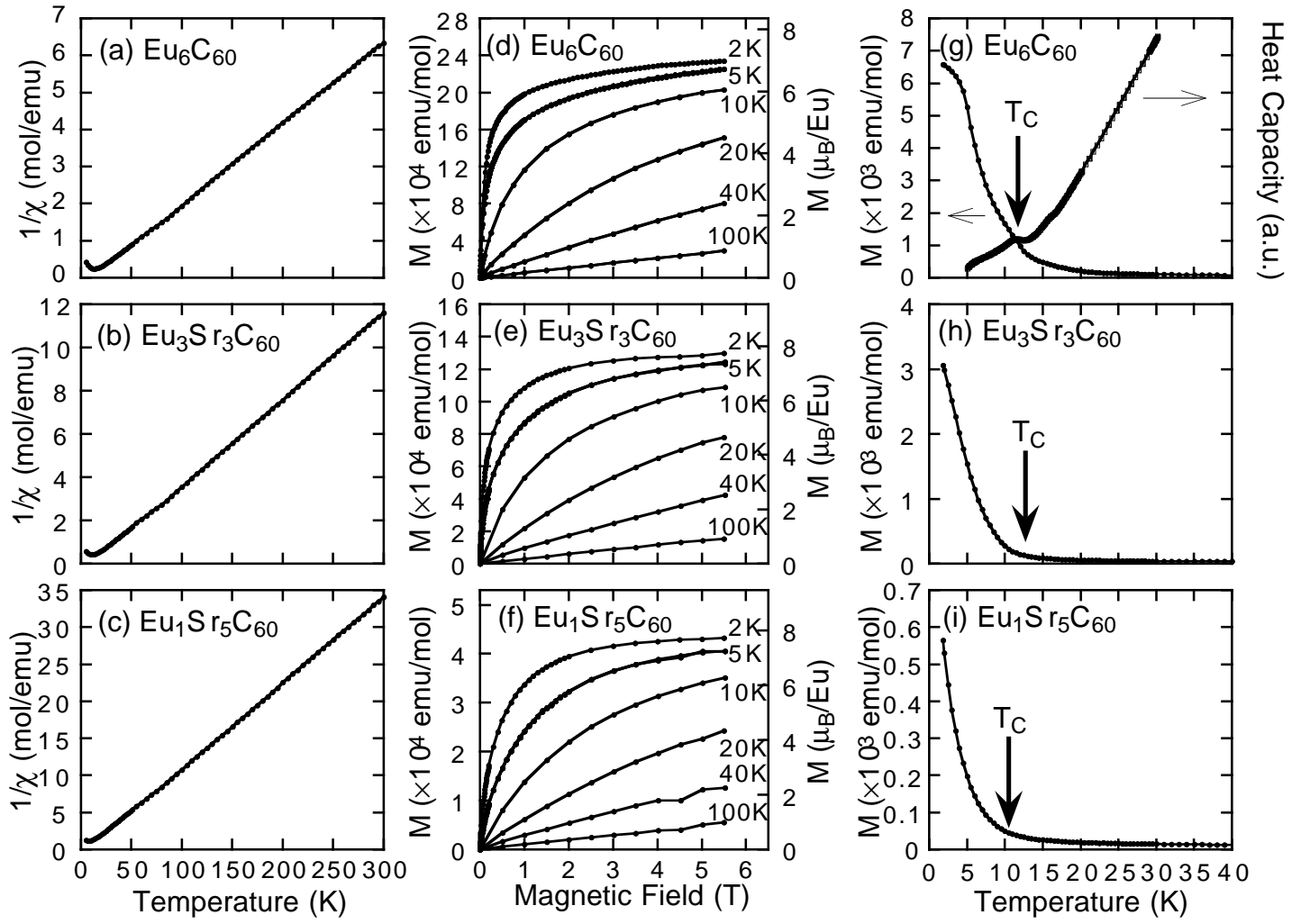


FIG. 2: (a)-(c) Inverse magnetic susceptibility obtained from the magnetization at 1 and 2 T. (d)-(f) Magnetization curve. (g)-(i) Temperature dependence of the magnetization at 3 mT. Heat Capacity of  $\text{Eu}_6\text{C}_{60}$  is also presented in (g). The arrows indicate the ferromagnetic transition temperatures determined the peak position of the heat capacity measurement for  $\text{Eu}_6\text{C}_{60}$ , and estimated from the Arrott plot for  $\text{Eu}_3\text{Sr}_3\text{C}_{60}$  and  $\text{Eu}_1\text{Sr}_5\text{C}_{60}$ .

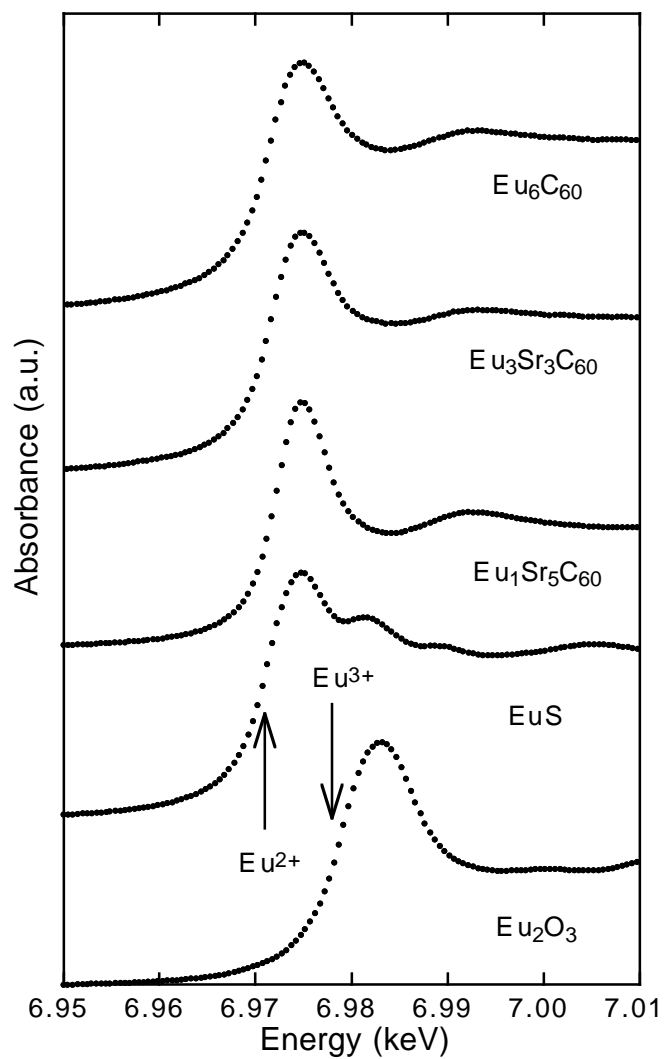


FIG. 3: XANES spectra of  $\text{Eu}_{6-x}\text{Sr}_x\text{C}_{60}$ . The arrows indicate the absorption edge in divalent and trivalent reference.



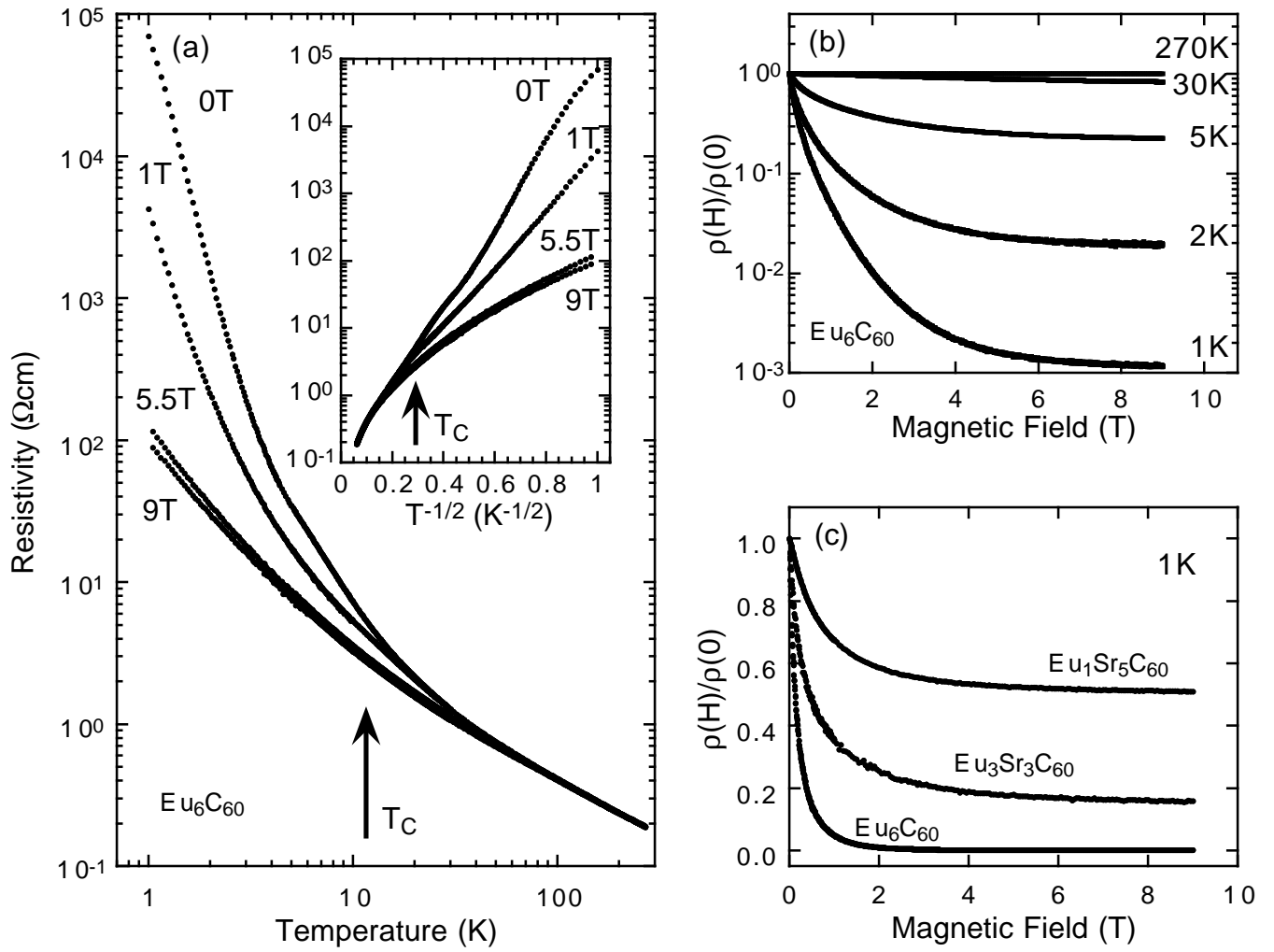


FIG. 4: (a) Temperature dependence of resistivity of polycrystalline Eu<sub>6</sub>C<sub>60</sub> at some magnetic fields. The arrow indicates the ferromagnetic transition temperature. (b) Magnetic field dependence of resistivity of Eu<sub>6</sub>C<sub>60</sub> normalized at zero field for some temperatures. (c) Magnetic field dependence of resistivity of Eu<sub>6-x</sub>Sr<sub>x</sub>C<sub>60</sub> normalized at zero field measured at 1 K.